Supplementary Information

Template-Free Synthesis of Functional Metal Oxide Nanotubes via Nonclassical Nucleation in a Continuous Injection Method

Mengxuan Zhang, [a, ‡] Ming Jiang,[a,‡] Zhongyao Bao,[a] Zisheng Feng,[a] Kun Han,[a] Tao Han,[a] ChenZhe Sun,[b] Yakun Zhou,[b] Chuanqiang Wu,[a,*] Zhen Huang,[a,b,*] Penghui Yin [a,*]

[a]*Anhui Provincial Key Laboratory of Magnetic Functional Materials and Devices, Institutes of Physical Science and Information Technology, Anhui University, Hefei 230601, China*

[b]*Stony Brook Institute at Anhui University, Anhui University, Hefei 230039, China*

*Corresponding author (Email: wucq@ahu.edu.cn; huangz@ahu.edu.cn; phyin@ahu.edu.cn)

‡These authors contributed equally.

Content:

I. Experimental Methods

Chemicals. Gallium acetylacetonate ($Ga(acac)_3$, 99%), ferrous acetylacetonate ($Fe(acac)_2$, 98%), hexacarbonyl tungsten ($W(CO)_6$, 97%), molybdenum acetylacetonate ($Mo(acac)_3$, 97%), chromium acetylacetonate ($Cr(acac)_3$, 98%), n-hexane (98%), and ethanol (99%), were purchased from Macklin. The oleyl alcohol (80-85%) and oleic acid (90%) was purchased from Alfa Aesar. All chemicals were used as received without additional purification.

Synthesis of Ga_2O_3 Nanotubes (NTs). The synthesis of γ-Ga_2O_3 nanostructures were based on a modified continuous growth method. Varying amount of $Ga(acac)_3$ (1, 2, and 3 mmol) was mixed with oleic acid (2 mL) and heated at 150 °C in an argon atmosphere for 30 minutes, resulting in a transparent, pale-yellow gallium oleate solution. Separately, in a 50 mL three-necked flask, oleyl alcohol (12.5 mL) was heated to 270 °C under a constant argon flow of 0.3 L/min. The oleate solution was injected using a 5 mL syringe and syringe pump with a controlled rate of 0.2 mL/min. After injection, the nanostructures were allowed to grow for an additional 20 minutes at 270 ℃, during which the color of reaction solution gradually transitioned from light yellow to intense yellow. Once the heating was completed, the solution was cooled to room temperature. The nanostructures were precipitated by adding ethanol and a small amount of deionized water into the solution followed by centrifugation at 7500 rpm for 30 minutes. The sample was washed with ethanol three times and dispersed in hexane for further characterizations.

To synthesize Ga_2O_3 NTs with mixed β and κ phases, the gallium oleate solution (1mmol in 2mL oleic acid) was injected into oleyl alcohol at 290 ℃ at a controlled rate of 0.01 mL/min, with subsequent procedure identical to those described above. For tuning the aspect ratio of Ga_2O_3 NTs, the injection rate of gallium oleate solution was modified by keeping the injection speed constant and adjusting the solution concentration. This was achieved by mixing 1 mmol $Ga(acac)_3$ with varying volumes of (1, 2, 3, and 4 mL) oleic acid, while all other experimental conditions remain unchanged. As a result, Ga_2O_3 NTs were synthesized with average lengths of 15.7 ± 3.0 nm, 31.4 ± 9.2 nm, 50.0 ± 13.9 nm, and 79.1 ± 21.9 nm, along with corresponding diameters of 2.5 ± 0.6 nm, 3.7 ± 0.7 nm, 5.0 ± 1.0 nm, and 5.4 ± 1.1 nm, as illustrated in Fig. 3 in the main text. Additionally, the injection rates were tuned by maintaining a constant concentration of gallium oleate solution and varying the injection speed to 0.04 mL/min, 0.02 mL/min and 0.01 mL/min. This yielded Ga_2O_3 NTs with average lengths of 24.6 ± 7.6 nm, 31.4 ± 9.2 nm, and 59.9 ± 17.1 nm, and diameters of 3.3 ± 1.1 nm, 3.7 ± 0.7 nm, 4.7 ± 0.8 nm, respectively, as shown in Fig. S17 of the supporting information.

To investigate reaction intermediates during synthesis at a gallium oleate solution injection rate of 0.005 mmol/min, 1 mL aliquots were extracted using a glass syringe at 25, 50, 75, 100, 150 and 200 minutes. After washing with the mixture of ethanol and water, the obtained reaction intermediates were dispersed in hexane for further analysis.

Synthesis of Representative Metal Oxide NTs.

Synthesis of Colloidal Fe_3O_4 NTs. $Fe(acac)_2$ (0.254 g, 1 mmol) was mixed with oleic acid (2 mL) and heated at 150 °C in an argon atmosphere for 30 minutes, resulting in a dark brown ferrous oleate solution. In a separate 50 mL three-necked flask, oleyl alcohol (12.5 mL) was heated to 290 °C under a constant argon flow of 0.3 L/min. The ferrous oleate solution was injected using a 5mL syringe and syringe pump with a controlled rate of 0.005 mmol/min. After injection, the NTs were allowed to grow for an additional 20 minutes at 290 °C. Upon completion of heating, the solution was cooled to room temperature, and the product was process identically to the Ga_2O_3 NTs.

Synthesis of Colloidal WO_{3-x} NTs. $W(CO)_6$ (0.3519 g, 1 mmol) was mixed with oleic acid (2 mL) and heated at 110 °C in an argon atmosphere for 30 minutes, resulting in a transparent, pale-yellow oleate solution. Separately, in a 50 mL three-necked flask, oleyl alcohol (12.5 mL) was heated to 290 °C under a constant argon flow of 0.3 L/min. The oleate solution was injected using a 5mL syringe and syringe pump with a controlled rate of 0.02 mmol/min. After injecting all oleate solution, The NTs were allowed to grow for an additional 20 minutes at 290 °C. The sample processing procedures were identical to those for the aforementioned metal oxide NTs.

Synthesis of Colloidal MoO_{3-x} and Cr_2O_3 Nanostructures. The molybdenum oleate solution was prepared by mixing $Mo(acac)_3$ (0.3262 g, 1 mmol) with oleic acid (2 mL) and heated at 150 °C in an argon atmosphere for 30 minutes, resulting in a dark brown solution. The chromium oleate solution was obtained by mixing $Cr(acac)_3$ (0.3493 g, 1 mmol) with

oleic acid (2 mL) and heated at 150 °C in an argon atmosphere for 30 minutes, yielding a deep green solution. The metal oleate solution was injected using a 5mL syringe and syringe pump with a controlled rate of 0.005 mmol/min. The nanostructures were allowed to grow for an additional 20 minutes at 290 °C after injection. The samples were processed identically to Ga_2O_3 NTs.

Characterization and Measurements. Powder X-ray diffraction (XRD) patterns were recorded utilizing a RIGAKU SmartLab-9KW diffractometer, equipped with a highly sensitive position-sensitive detector and monochromatic Cu Kα radiation (λ = 1.5418 Å). To obtain the powder samples, the NTs were precipitated by adding ethanol into hexane suspension and followed by centrifugation. Transmission electron microscopy (TEM) overview images were captured using a JEM-2100 microscope operating at 200 kV. For TEM measurements, the specimens were prepared by drop casting diluted colloidal NC suspensions in toluene onto copper grids coated with ultrathin carbon support films. The Scanning TEM images were collected using a JEOL NEOARM microscope. The absorption spectra of various Ga_2O_3 NTs, prepared as colloidal dispersions in hexane, were measured using a Hitachi UH5700 UV-vis-NIR spectrophotometer. The Cary Eclipse fluorescence spectrometer was used to record the photoluminescence (PL) emission spectra. The NT suspension in hexane was excited at 250 nm to obtain these spectra. Delayed PL spectra were collected under the same excitation, with a delay time of 0.1 ms and a gate time of 4.5 ms. To monitor the microsecond PL lifetime, measurements were taken at the

peak wavelength of the delayed PL spectra with an initial delay of 1 μs and an excitation of 250 nm. Fourier transform infrared (FTIR) spectra of Ga_2O_3 NT reaction intermediates were recorded using a Bruker Vertex 80 spectrometer. Powder samples were mixed with KBr in approximately 1:50 weight ratio and pressed into pellets for the FTIR measurement. Magnetization data were measured using a Magnetic Property Measurement System (MPMS3, Quantum Design). The measurements were taken at 300 K and magnetic fields of 0−1T. For magnetization measurements of free-standing NTs, the colloidal NC samples were precipitated with ethanol, dried, and loaded into sample capsules.

X-ray absorption fine structure (XAFS) analyses of the Ga L_3-edge were conducted utilizing a commercial Laboratory-Based XAFS spectrometer (Rapid XAFS 2M, Anhui Absorption Spectroscopy Analysis Instrument Co., Ltd.). X-rays were generated via a Mo target X-ray source operated at 20 kV and 20 mA. A Si (840) spherically bent crystal analyzer (SBCA) with a radius of curvature of 500 mm served as the monochromator, thereby ensuring a diffraction geometry approaching a 90-degree backscatter angle at the absorption edge. After monochromatization, the X-rays pass through the sample and were collected using a high-energy-resolution silicon drift detector (SDD) to obtain the X-ray intensity. The XAFS data were acquired in transmission mode. During the XAFS measurements, the position of the absorption edge (E_0) was calibrated using a standard Ga_2O_3 sample, and all data collection occurred within a single time period.

Computational Method. All the calculations were performed within the framework of density functional theory (DFT) utilizing the projector augmented wave method, as implemented in the Vienna *Ab Initio* Simulation Package (VASP). Projector augmented-wave pseudopotentials to model the interaction between ions and electrons and the exchange-correlation effects were accounted for using the Perdew-Burke-Ernzerhof (PBE) functional under the generalized gradient approximation (GGA). For the bond dissociation energy calculations, a 4×4×1 Monkhorst-Pack grid of *k*-points and the kinetic energy cutoffs of 450 eV was used. All the atoms were optimized until the total energies converged to below 10^{-4} eV and the forces acting on atoms were less than 10^{-3} eV/Å. Generally, the bond dissociation energy is defined as the electronic structure energy change of the following reaction in the vacuum $A-B=A.+B.$ in which A and B represent the two fragments formed by breaking the A-B covalent bond in a molecule. After the geometry was optimized for the molecule, the target bond was cut and the molecule was broken into two separate fragments. Generally, the radial distribution function (RDF) is the variations of neighboring matter density as a function of distance, which is defined by the following equation,

$$g(r)=\frac{1}{4\pi r^2 \rho N}\sum_{i=1}^{N}\sum_{j\neq 1}<\delta(r-r_{ij})>$$

Here, r is the radial distance from a reference particle. N is the total number of particles in the system. V is the system volume. r_{ij} is the distance between particle i and particle j. For the ab-initio molecular dynamics (AIMD) calculations for determining

the RDF of Ga_2O_3, a compromise is made between computation efficiency and accuracy, resulting in the usage of a cut-off energy of 400 eV for the basis set and a 1 × 1 × 1 Monkhorst-Pack *k*-point sampling in the Brillouin zone. The VESTA package was used to visualize the various structures.

II. Supporting Figures

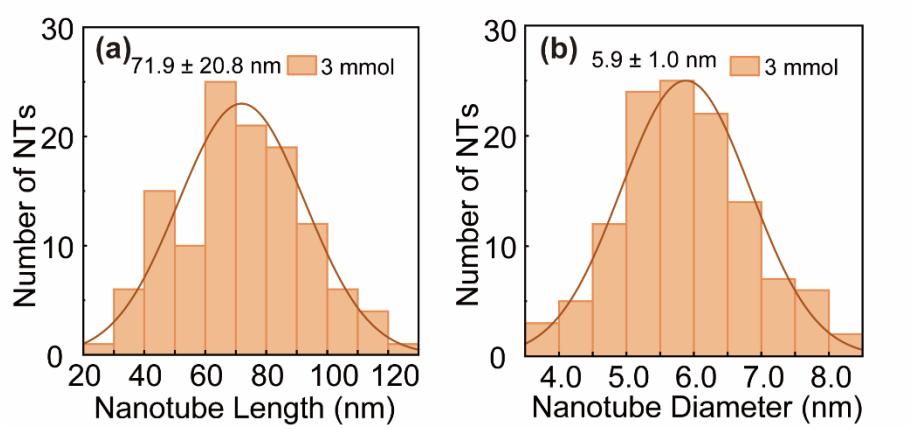

Figure S1. Size distribution histogram of NT (a) length and (b) diameter for Ga_2O_3 NT sample shown in Figure 1c in the main text.

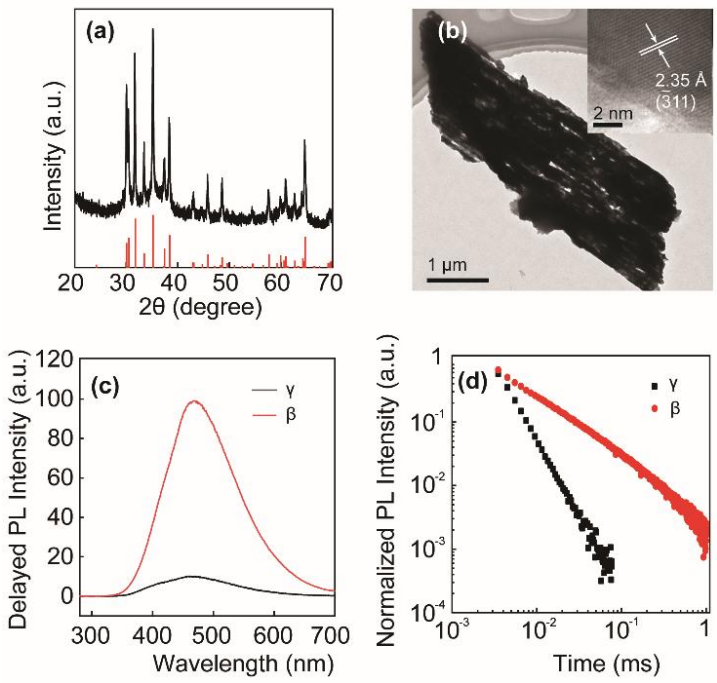

Figure S2. (a, b) The XRD pattern (a) and overview TEM image (b) of β-Ga_2O_3 sample obtained by size-selective precipitation. Red vertical lines in panel a correspond to the reference pattern of monoclinic Ga_2O_3 (JCPDS 076-0573). The inset in panel b shows the high-resolution TEM image of an isolated β-Ga_2O_3 sample. The measured lattice fringes are 2.35 Å, which agrees well with the β-Ga_2O_3 ($\bar{3}11$) interplanar lattice spacing. (c, d) Normalized delayed PL spectra (c) and time-resolved PL intensities (d) of the β-Ga_2O_3 sample in b and Ga_2O_3 NCs synthesized with 1 mmol gallium precursor, as indicated in the graph. Delayed PL spectra were collected under the excitation at 250 nm, with a delay time of 0.1 ms and a gate time of 4.5 ms. The spectra were normalized to the band gap absorption for a reasonable comparison. To monitor the microsecond PL lifetime, measurements were taken at the peak wavelength of the delayed PL spectra with an initial delay of 1 μs and an excitation of 250 nm.

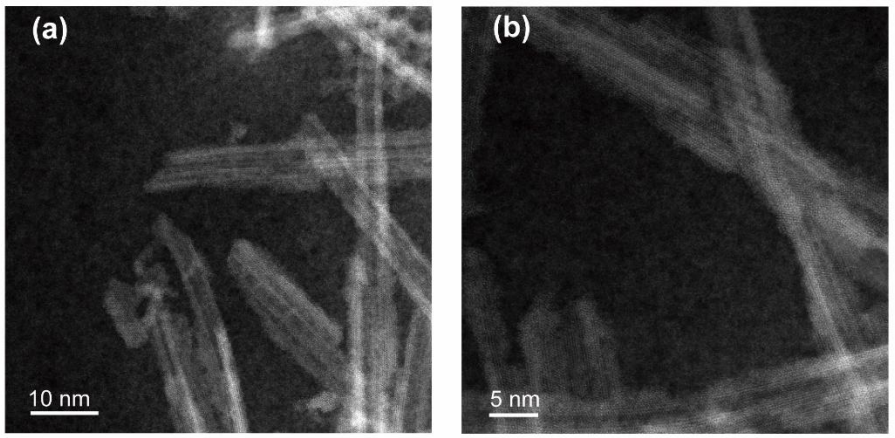

Figure S3. (a, b) The overview dark field TEM images of γ-Ga_2O_3 NT sample shown in Figure 1c in the main text.

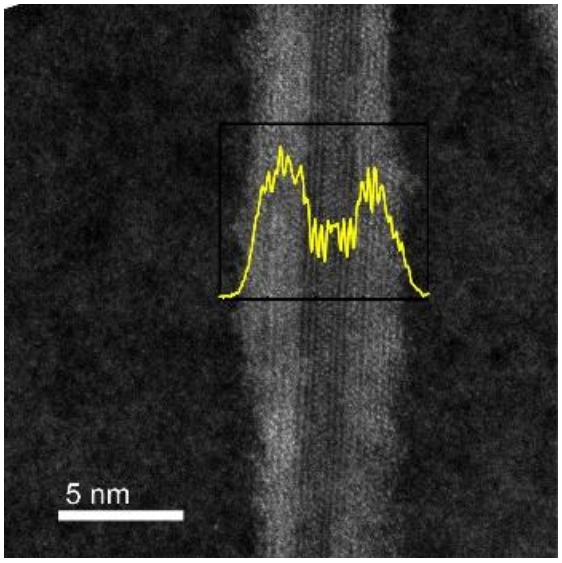

Figure S4. The line scan intensity across the radial direction of a single γ-Ga_2O_3 NT.

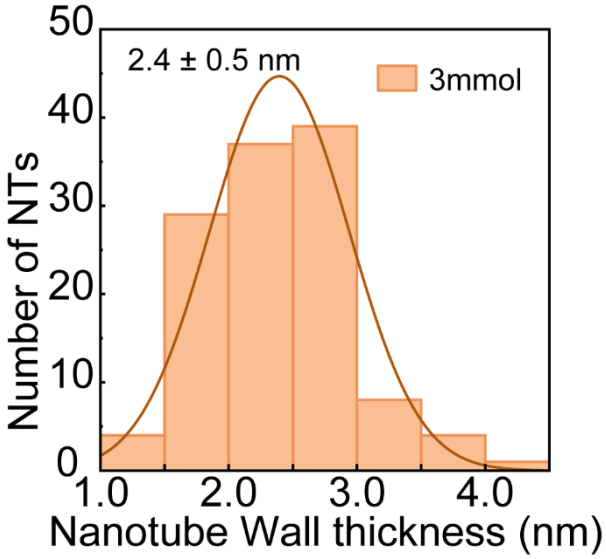

Figure S5. The size distribution histograms of NT wall thickness for Ga_2O_3 NTs shown in Figure 1c of the main text.

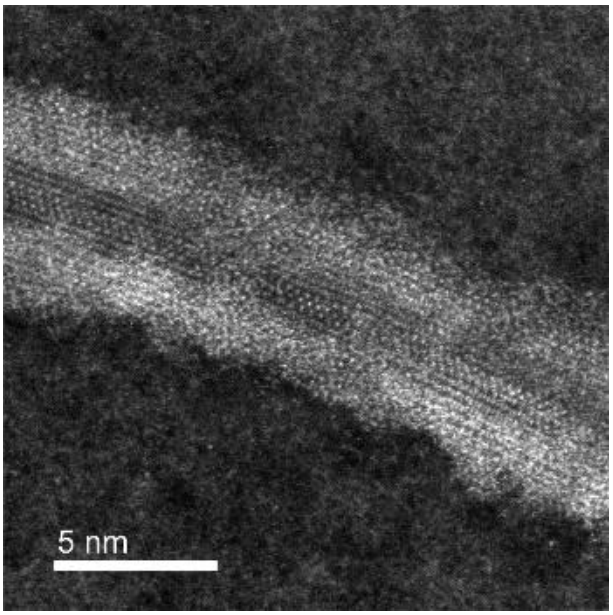

Figure S6. The HAADF image of a single γ-Ga_2O_3 NT. The FFT of this image was shown in Figure 1g in the main text.

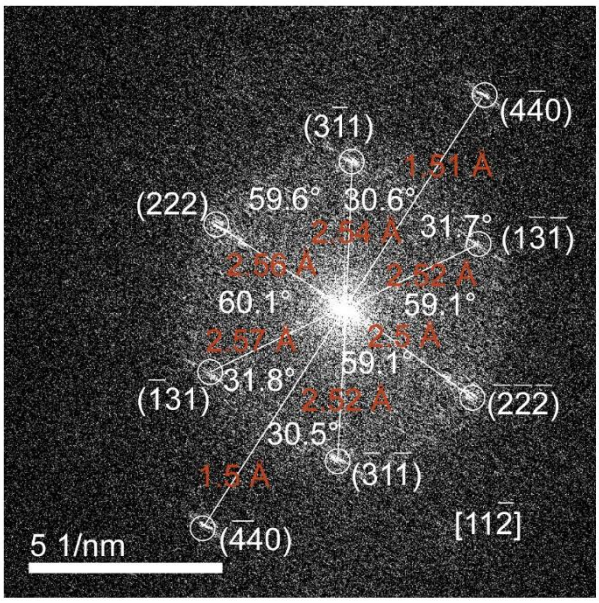

Figure S7. The measured distances and angles among the spots in the FFT pattern depicted in Figure 1g in the main text, along with the identification of lattice planes for γ-Ga_2O_3 aligned along the $[11\bar{2}]$ zone axis.

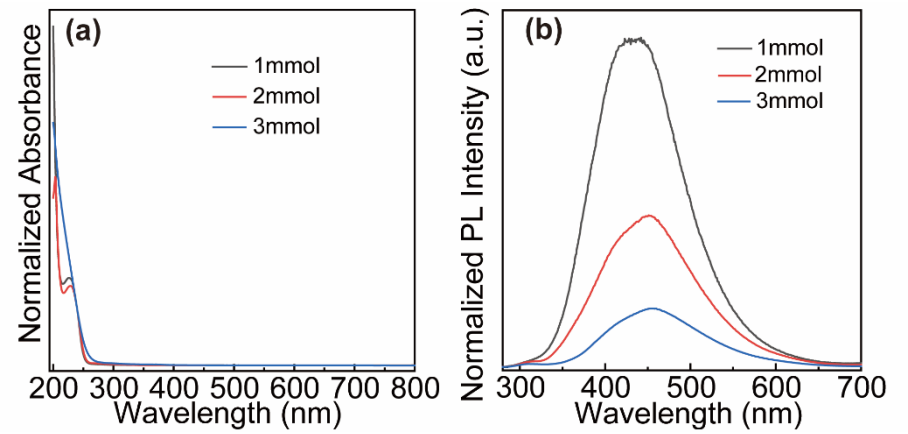

Figure S8. (a) Normalized optical absorption spectra (b) and normalized PL spectra of Ga_2O_3 nanostructures synthesized various amount of gallium precursor, as indicated in the graph.

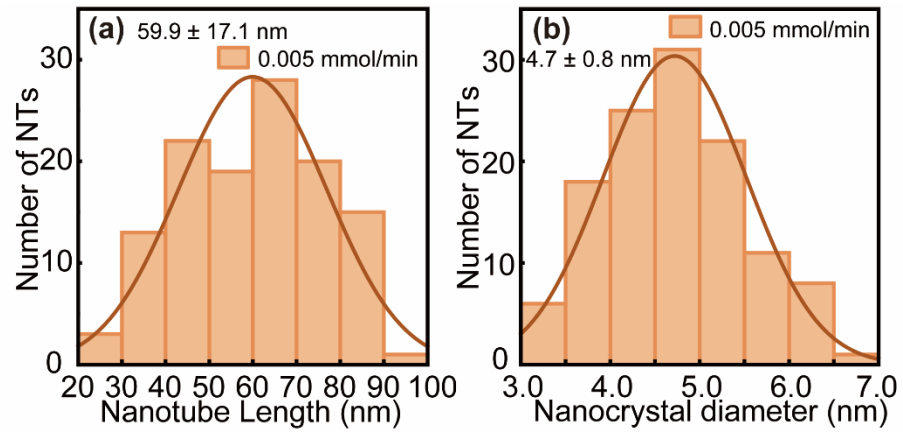

Figure S9. Size distribution histogram of NT (a) length and (b) diameter for Ga_2O_3 NT sample synthesized at a gallium oleate solution injection rate of 0.005 mmol/min.

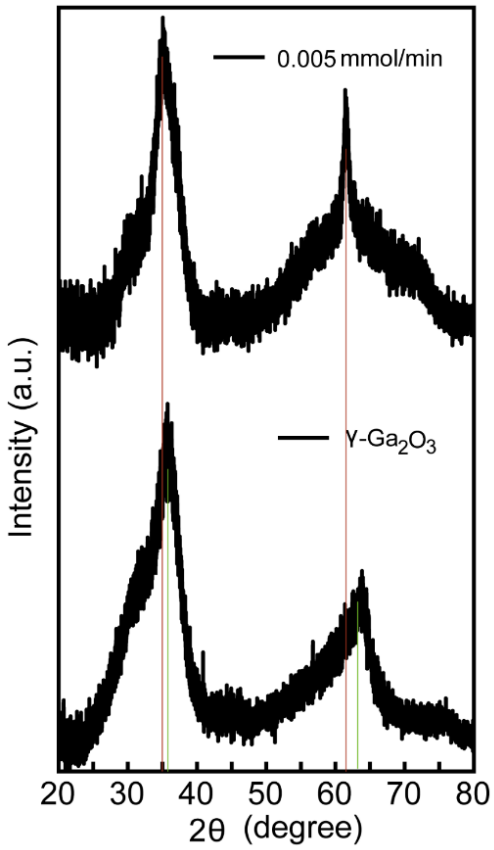

Figure S10. The comparison of XRD patterns of Ga_2O_3 NT samples synthesized at a gallium oleate solution injection rate of 0.005mmol/min, alongside with that of γ-Ga_2O_3 NCs. The light red and green vertical lines highlight the shifts of diffraction peaks.

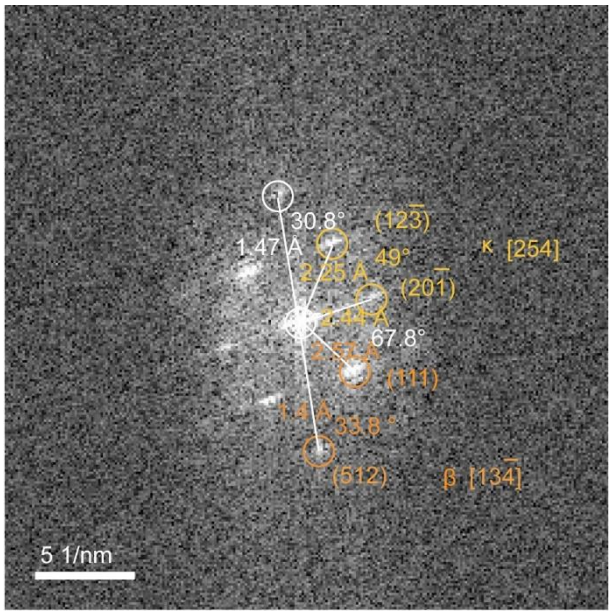

Figure S11. The measured distances and angles among the spots in the FFT pattern depicted in Figure 2c in the main text, along with the identification of lattice planes for β- and κ-Ga_2O_3.

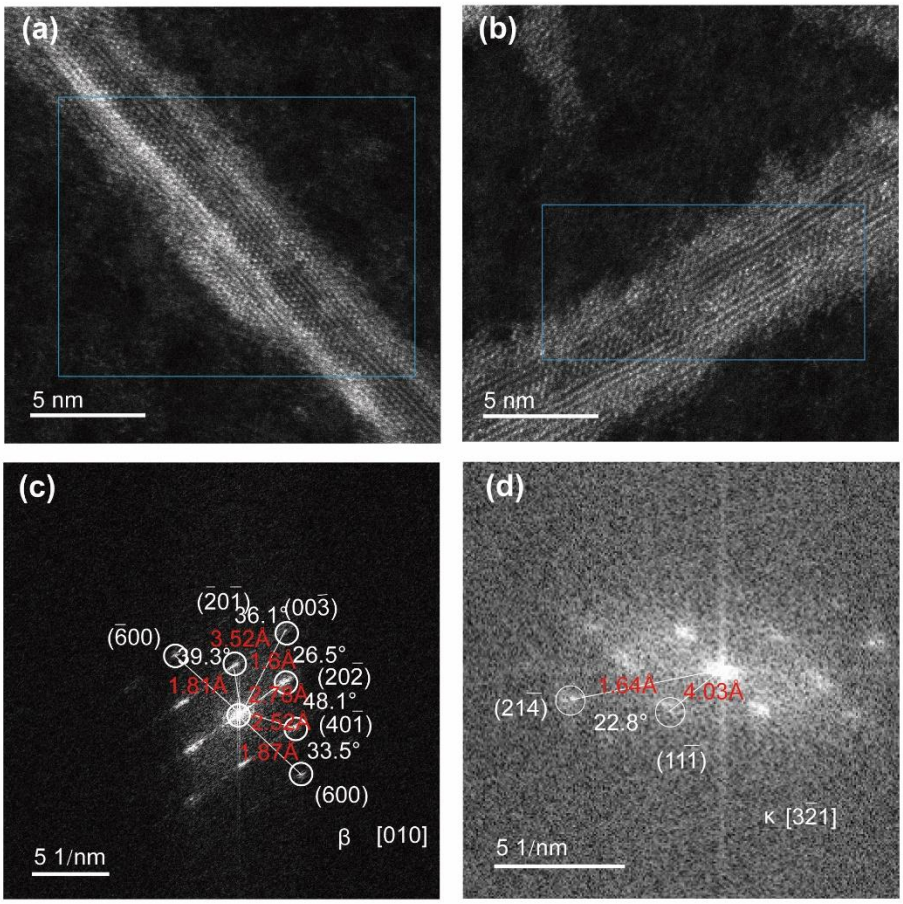

Figure S12. (a, b) The HAADF images of additional isolated Ga_2O_3 NTs, synthesized at a gallium oleate solution injection rate of 0.005 mmol/min. (c, d) FFT analysis of the NT segments shown in the panels a and b, with the regions of interest marked by blue boxes. The measured distances and angles between the spots in panels c and d are annotated, accompanied by the assignment of corresponding lattice planes for β- and κ-Ga_2O_3 phases.

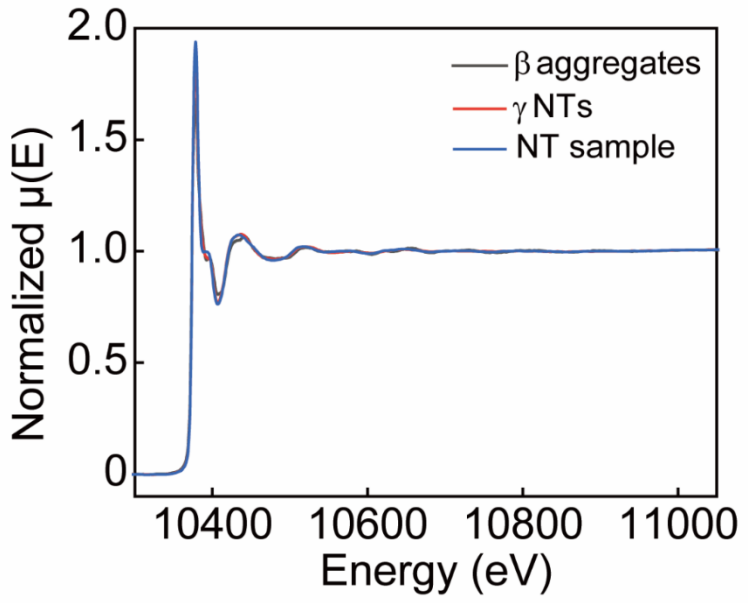

Figure S13. The EXAFS spectra of Ga_2O_3 NT sample synthesized at a gallium oleate solution injection rate of 0.005 mmol/min (blue trace), in comparison with γ-Ga_2O_3 NTs (red trace) and β-Ga_2O_3 aggregates (black trace).

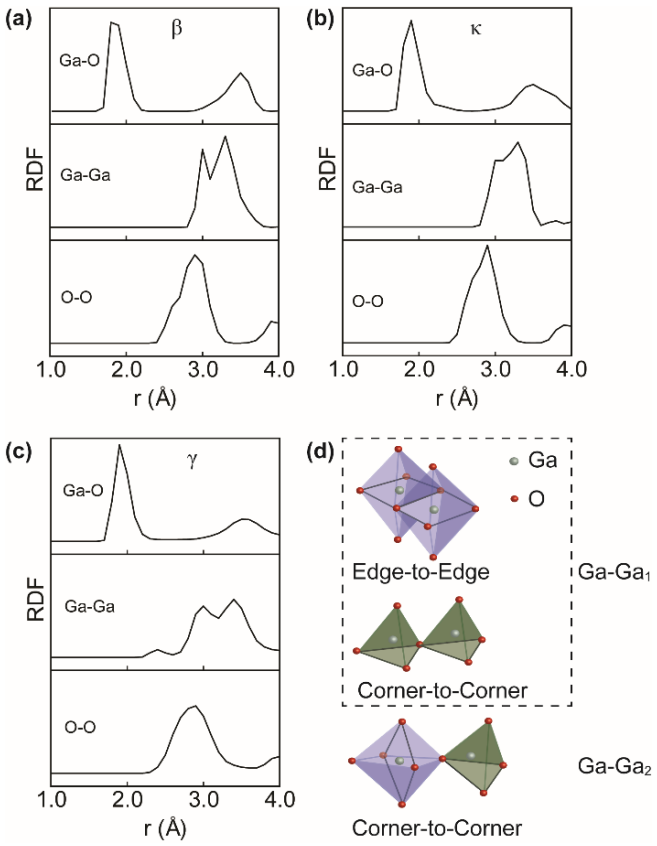

Figure S14. (a, b, c) The simulated radial distribution functions of (a) β-, (b) κ- and (c) γ-Ga_2O_3. For the calculation of κ- and γ-Ga_2O_3, the crystal structures used were based on reference 48 and 42 in the main text, respectively. (d) Schematic representations of two different Ga-Ga pairs with different arrangements of octahedral and tetrahedral units. The gray and red spheres represent gallium and oxygen atoms, respectively.

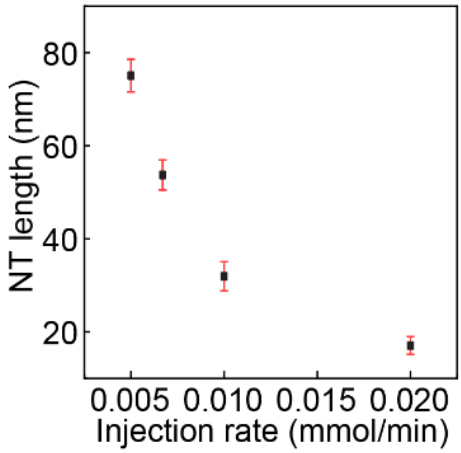

Figure S15. Mean NT length as a function of injection rates used in the experiments as described in the main text.

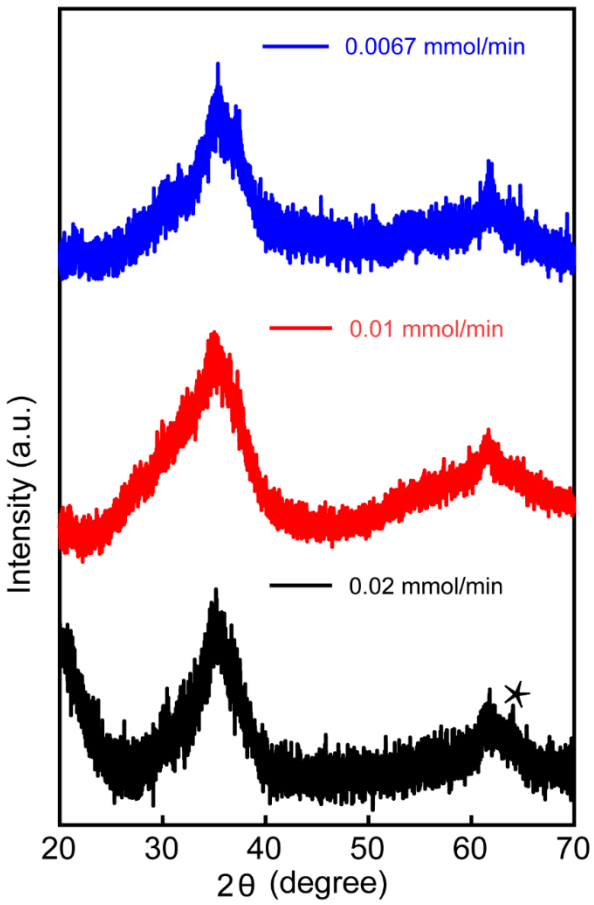

Figure S16. The XRD patterns of Ga_2O_3 NT samples synthesized with various gallium oleate solution injection rate, as indicated in the graph. The diffraction peak of γ-Ga_2O_3 is denoted with an asterisk.

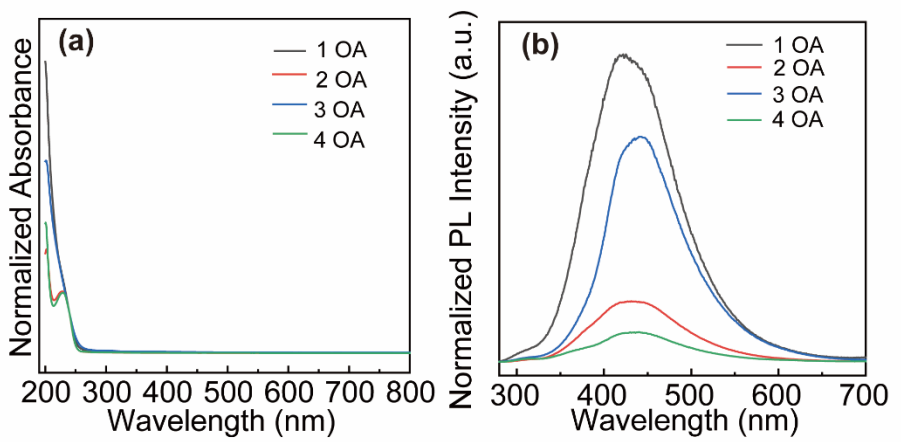

Figure S17. (a) Normalized optical absorption spectra and (b) normalized PL spectra of Ga_2O_3 NTs synthesized at various injection rate of gallium oleate solution, as indicated in the graph. The PL emission was collected under the excitation at 250 nm.

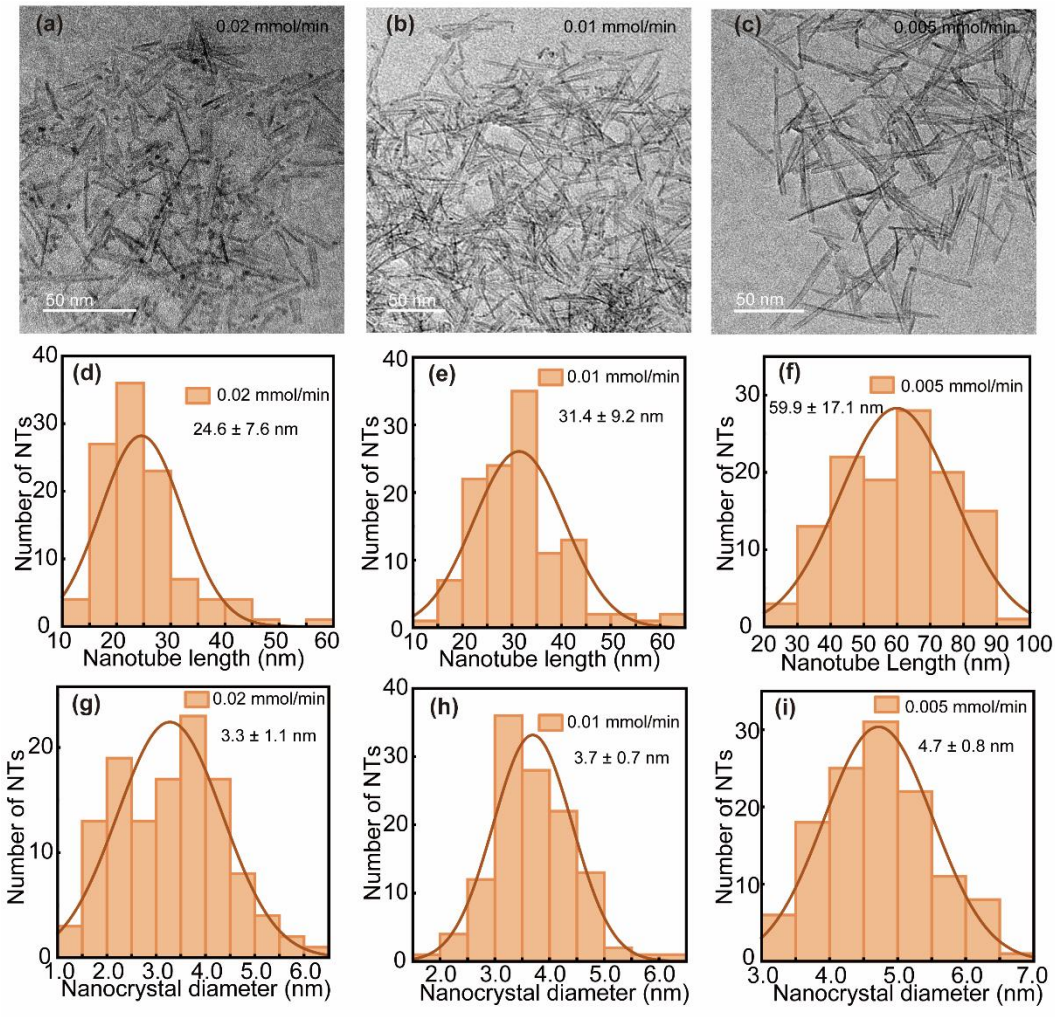

Figure S18. (a, b, c) The overview TEM images of Ga_2O_3 NTs synthesized at various injection rate of gallium oleate solution, as indicated in the graph. The injection rates were adjusted by maintaining a constant concentration of gallium oleate solution while altering the injection speed of the solution. Correspondingly, the size distribution histograms of NT length (d, e, f) and diameter (g, h, i) are summarized for each synthesis condition.

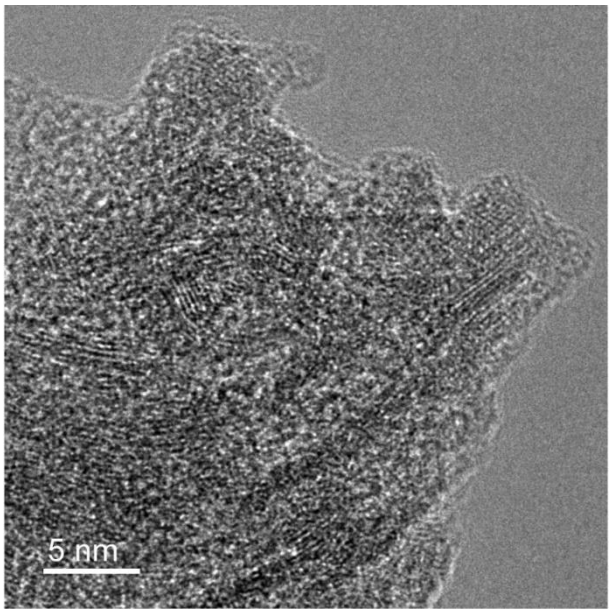

Figure S19. The HRTEM image of the bundled thin nanofiber extracted at 50 minutes of reaction time, under the condition that the gallium oleate solution was injected at a rate of 0.005 mmol/min.

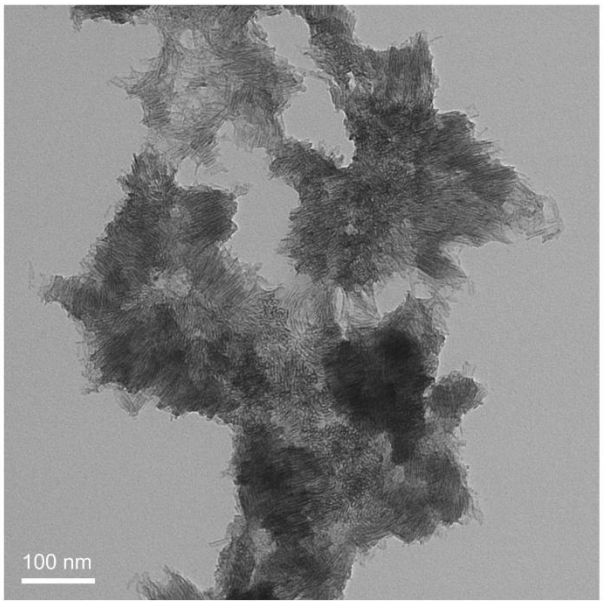

Figure S20. The overview TEM image of Ga_2O_3 nanofiber bundles collected at 75 minutes of reaction time, under the condition that the gallium oleate solution was injected at a rate of 0.005 mmol/min.

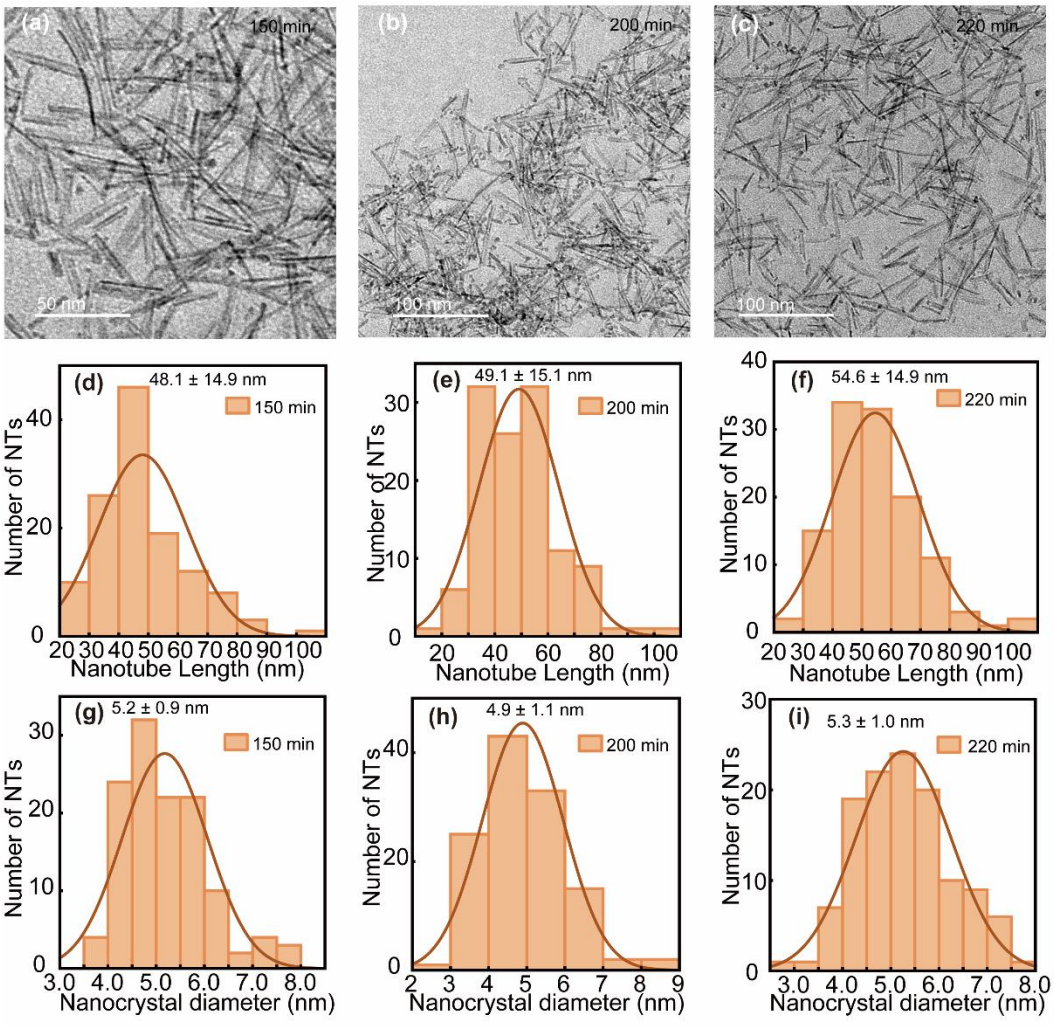

Figure S21. (a, b, c) The overview TEM images of Ga_2O_3 NTs collected at (a) 150 minutes, (b) 200 minutes, and (c) 220 minutes of reaction time, under the condition that the gallium oleate solution was injected at a rate of 0.005 mmol/min. Correspondingly, the size distribution histograms of NT length (d, e, f) and diameter (g, h, i) were summarized for each sample.

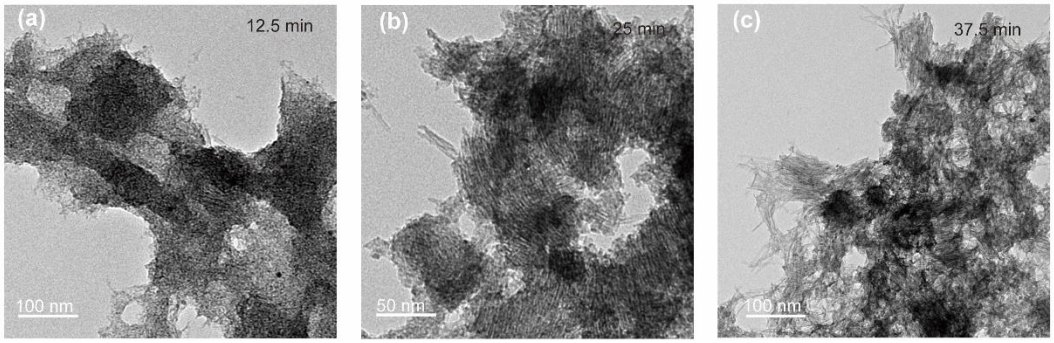

Figure S22. The overview TEM images of reaction intermediates extracted at (a) 12.5 minutes, (b) 25 minutes, and (c) 37.5 minutes of the reaction time, under the condition that the gallium oleate solution was injected at a rate of 0.01 mmol/min.

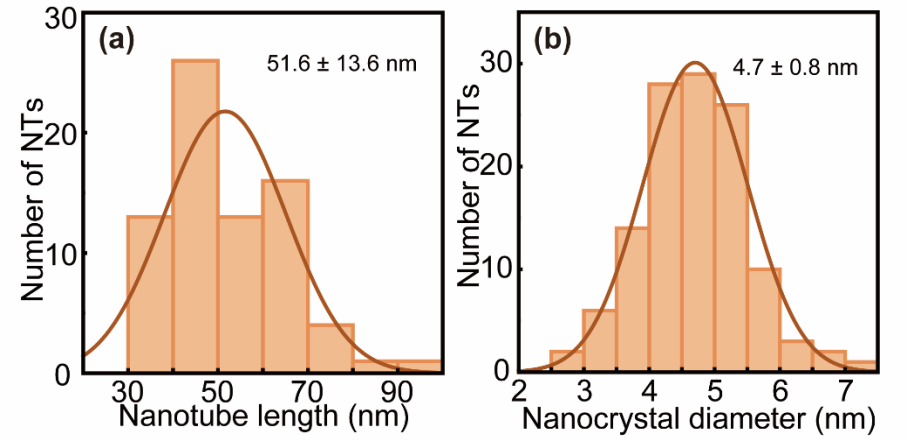

Figure S23. Size distribution histogram of NT (a) length and (b) diameter for Fe_3O_4 NT sample shown in Figure 5a in the main text.

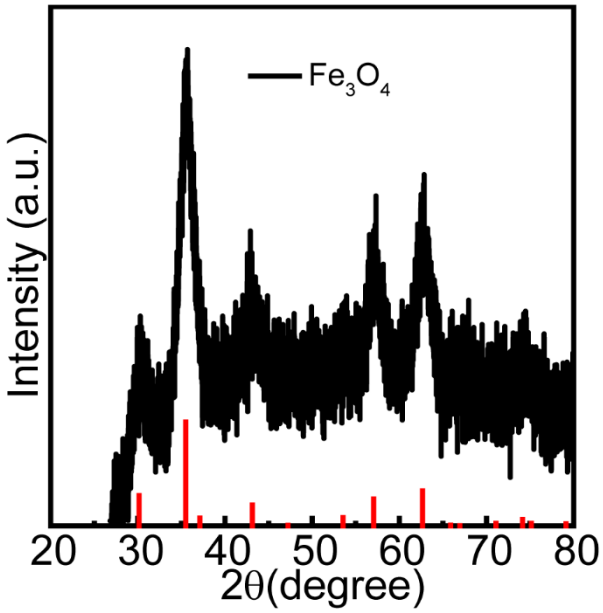

Figure S24. XRD pattern of Fe_3O_4 NT sample. Red vertical lines correspond to the XRD pattern for cubic Fe_3O_4 (JCPDS 089-0691).

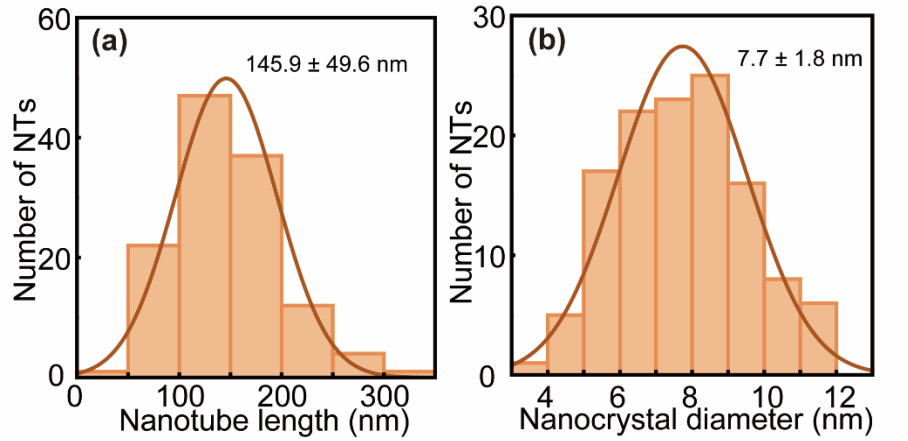

Figure S25. Size distribution histogram of NT (a) length and (b) diameter for WO_{3-x} NT sample shown in Figure 5c in the main text.

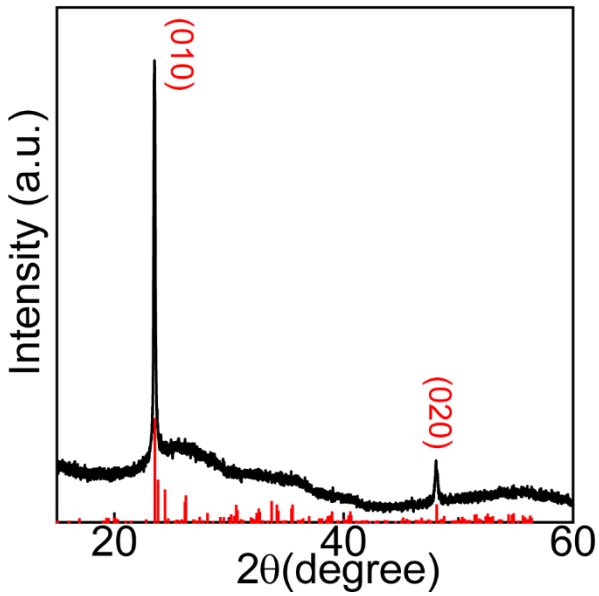

Figure S26. The XRD pattern of WO_{3-x} NT sample. Red vertical lines correspond to the XRD pattern for monoclinic $W_{18}O_{49}$ (JCPDS 084-1516).

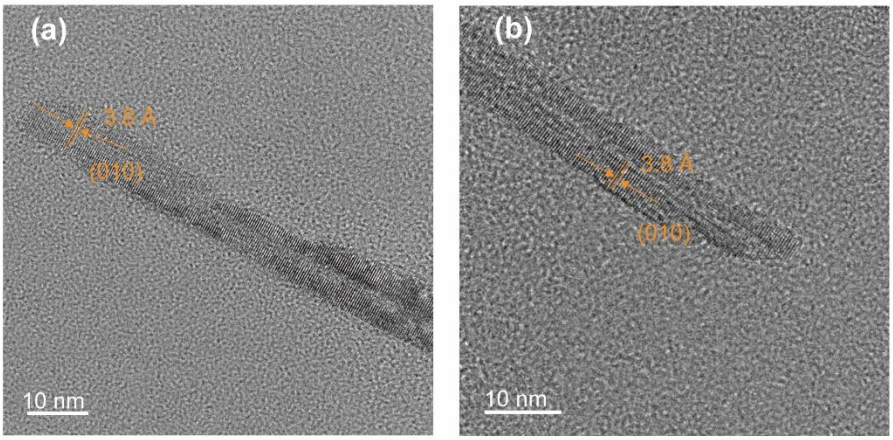

Figure S27. (a, b) High-resolution TEM image of isolated WO_{3-x} NTs. The measured lattice fringes are 3.8 Å, which agrees well with the $W_{18}O_{49}$ (010) interplanar lattice spacing.

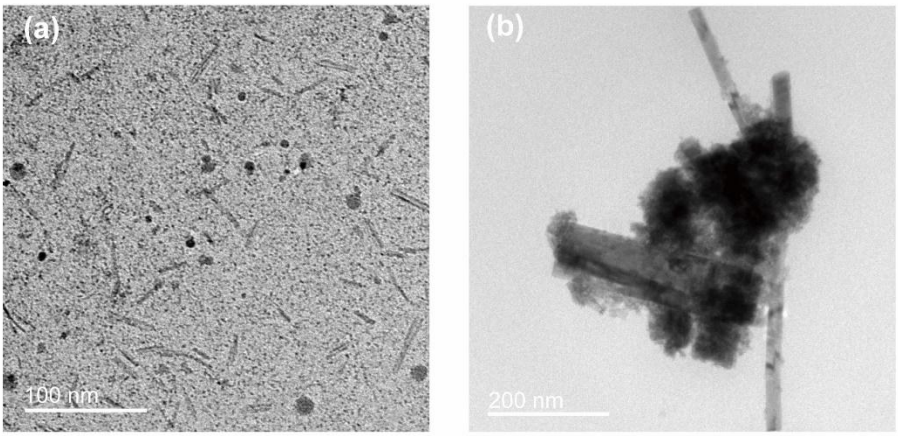

Figure S28. The overview TEM images for (a) MoO_{3-x} and (b) Cr_2O_3 nanostructures, synthesized under experimental conditions mirroring those employed for the synthesis of Ga_2O_3 NTs.

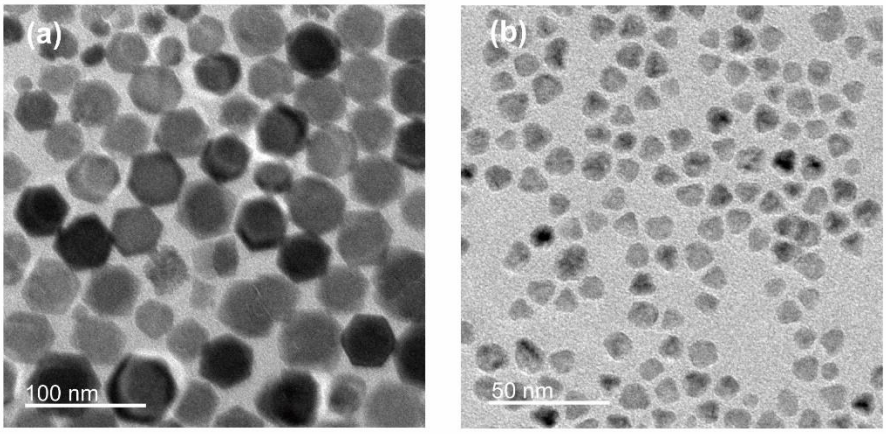

Figure S29. The overview TEM images for (a) In_2O_3 NCs and (b) Mn_3O_4 NCs synthesized utilizing experimental conditions analogous to those employed for the fabrication of Ga_2O_3 NTs.

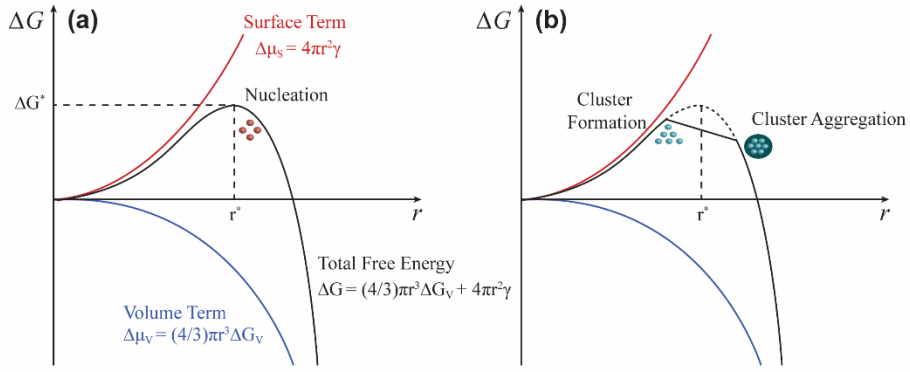

Figure S30. Schematic representations of the change of volume free energy, $\Delta\mu_v$, surface free energy, $\Delta\mu_s$, and total free energy, ΔG, as functions of nucleus's radius for (a) classical nucleation and (b) nonclassical nucleation.

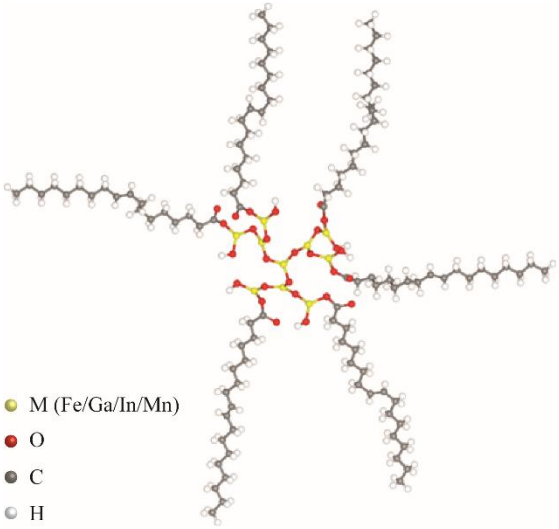

Figure S31. The full molecular structure of the metal oxide cluster shown in the Figure 6b in the main text. The yellow, red, gray, and white spheres represent metal, oxygen, carbon, and hydrogen atoms, respectively.

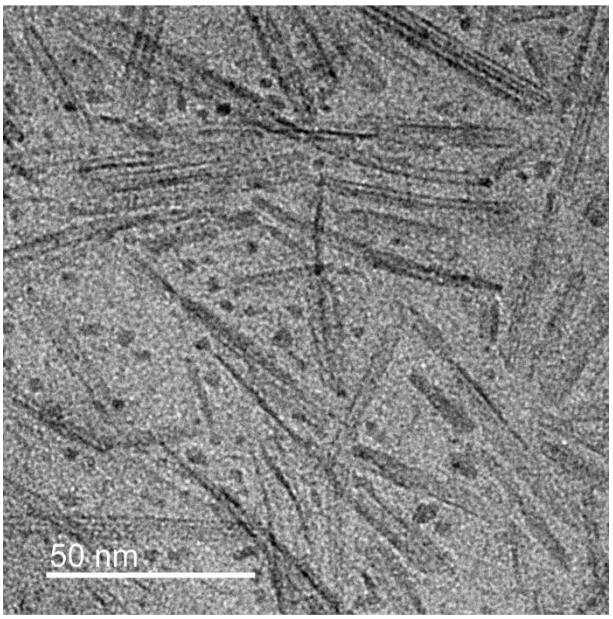

Figure S32. The overview TEM images for Ga_2O_3 nanostructures synthesized under the condition that the gallium oleate solution was injected at a rate of 0.1 mmol /s.